LAWRENCE
LIVERMORE
NATIONAL
LABORATORY

LLNL-JRNL-554312

An arbuscular mycorrhizal fungus modifies the soil microbial community and nitrogen cycling during litter decomposition

E. E. Nuccio, A. Hodge, J. Pett-Ridge, D. J. Herman, P. Weber, M. K. Firestone

May 2, 2012

Environmental Microbiology

Disclaimer

LLNL-JRNL-554312

An arbuscular mycorrhizal fungus modifies the soil microbial community and nitrogen cycling during litter decomposition

Erin E. Nuccio

Angela Hodge

Jennifer Pett-Ridge

Donald J. Herman

Peter Weber

Mary K. Firestone

ABSTRACT

Microbes are critical drivers of terrestrial biogeochemical processes and are mediators of soil organic matter stabilization. The arbuscular mycorrhizal fungal (AMF) symbiosis is often acknowledged for its role in plant nutrient capture, yet little is known about the interactions between AMF and the soil microbial community during nutrient uptake. We tested whether the AMF *Glomus hoi* alters the soil microbial community during litter decomposition, and we used ^{13}C and ^{15}N tracers to identify possible mechanisms governing the interactions between the AMF and the saprotrophic microbial community. Approximately 10% of the bacterial community in decomposing litter responded to AMF, and these taxa exhibited significant patterns of phylogenetic dispersal. The AMF also exported 5% of the litter-N to the host plant, and reduced the C:N of the litter remaining in the soil. We propose that export of N from litter is one mechanism by which AMF modify the composition of bacteria in decomposing litter. As approximately two-thirds of all land plants form associations with AMF, the effect of AMF on litter decomposition and N transfer is expected to be widespread and globally relevant for terrestrial biogeochemical cycling.

INTRODUCTION

The arbuscular mycorrhizal (AM) association between Glomeromycota fungi and land plants is widespread and ancient, and it is thought that this symbiosis enabled plants to colonize land (Remy *et al.* 1994; Brundrett 2002). AM fungi (AMF) are obligate symbionts that depend on their host plant for carbon nutrition and are not saprotrophic (Parniske 2008; Leigh *et al.* 2011; Smith & Smith 2011). However, AMF hyphae commonly proliferate in decomposing organic material (Nicolson 1959; St. John *et al.* 1983). In one study, AMF preferentially colonized soil amended with plant litter instead of an additional host plant, which represented a potential new carbon source (Hodge *et al.* 2001). In addition, AMF have been shown to stimulate the decomposition of plant material (Hodge *et al.* 2001; Atul-Nayyar *et al.* 2009), although the mechanism of this effect is unknown. As soil microbial communities mediate many biogeochemical processes in soil, it is likely that AMF alter decomposition by influencing the saprotrophic microbial community. Changes in microbial community composition can alter the production of bioactive metabolites and decomposition processes, and ultimately affect long-term carbon stabilization (Schmidt *et al.* 2011). Since approximately 80% of all land plants form symbiotic associations with AMF (Smith & Smith 2011), the effects of AMF on litter decomposition are expected to be globally relevant for terrestrial biogeochemical cycling (Hodge & Fitter 2010).

An essential function of the AMF symbiosis is the bidirectional exchange of nutrients between the host plant and fungal symbiont. AMF enhance nutrient acquisition for the host plant by transferring phosphorus (P) captured from soil in exchange for carbon (C) derived from photosynthate (Smith & Smith 2011). Relatively recently, AMF have been found to transfer nitrogen (N) to the host plant from decomposing litter (Hodge *et al.* 2001; Hodge & Fitter 2010).

In one study, the AMF acquired approximately one third of the N from decomposing litter and exported 3% of the litter-N to the host plant (Hodge & Fitter 2010), and in another study up to one third of the litter-N was exported to the host plant (Leigh *et al.* 2009). AMF are also large sinks for photosynthate (Johnson *et al.* 2002), and can supply C beyond the rooting zone to decomposing litter (Herman *et al.* 2012). The composition of hyphal exudates have been reported to contain low molecular-weight sugars and organic acids, as well as unidentified high molecular-weight polymeric compounds (Toljander *et al.* 2007). These compounds are energy rich, and may have a stimulatory effect on the surrounding microbial community (Toljander *et al.* 2007). In addition, as extraradical hyphae have a fast C turnover (Staddon *et al.* 2003), AM hyphae could be an important form of substrate.

Despite the important functions of the AM symbiosis, we still know comparatively little about the AM fungi and their interactions with other soil microorganisms (Hodge & Fitter 2010). In the rhizosphere, which is the soil immediately adjacent to plant roots, plant growth-promoting rhizobacteria (PGPRs) have been studied extensively in the tritrophic plant-AMF-bacterial interaction (Frey-Klett *et al.* 2007). The influence of AMF on soil microbial communities beyond the rhizosphere is largely unknown, even though extraradical hyphae are the main zone of interaction between AMF and the soil microbial community (Toljander *et al.* 2007). As the soil surrounding hyphae is difficult to assay directly in soil, *in vitro* studies using split plates and soil filtrates have been used to study bacterial attachment to surface of the hyphae (Toljander *et al.* 2007; Scheublin *et al.* 2010), as well as to examine the effect of AMF exudates on bacterial and fungal isolates (Filion *et al.* 1999). Some studies have found that AMF may repress members of the microbial community (Green *et al.* 1999; Welc *et al.* 2010), or may be repressed themselves by the other microbes (Leigh *et al.* 2011). Few studies have explicitly studied the

influence of AMF on the soil microbial communities in decomposing litter. Two previous studies using phospholipid fatty acids (PLFA) found that AMF had no discernable effect on the composition of the microbial community present in litter-containing soil, but this technique only detects gross changes in microbial community composition (Hodge et al. 2001, Herman et al. 2012). No previous studies have investigated how AMF impact the microbial communities using molecular techniques with high phylogenetic resolution.

A previous study of this plant-soil-mycorrhizal system has indicated that bacteria, rather than fungi, are the primary processors of litter-derived C during the intermediate and late stages of decomposition, while fungi are prominent processors during the early stages of decomposition (Herman *et al.* 2012). We hypothesized that (1) the presence of AMF will modify the bacterial communities in decomposing litter, and that (2) the mycorrhizal fungus will alter the physiochemical environment for the microbial community by exporting N from the decomposing litter. The aim of this study was to identify potential AMF-mediated mechanisms that drive changes in soil microbial communities associated with decomposing litter.

METHODS

Experimental Set-Up. Plants were grown in microcosm units constructed by connecting two plastic boxes (13.5 x 14.0 x 14.0 cm) via a double-mesh barrier (Figure 1). The planted chamber contained *Plantago lanceolata* L.—a plantain common to cultivated land—inoculated with the AMF *Glomus hoi* (University of York isolate #110). The litter chamber contained loam soil mixed with dried ^{13}C-only or ^{13}C and ^{15}N dual-labelled *P. lanceolata* root litter. Units with a 20 μm mesh barrier (John Stanier & Co., Whitefield, Manchester, UK) allowed hyphae to pass into the litter chamber, but excluded plant roots (Figure 1A). Units with 0.45 μm mesh (Anachem, Bedfordshire, UK) excluded hyphae from the litter chamber but permitted solute diffusion between the chambers (Figure 1B). In total, 50 dual-chamber units were established: 2 treatments with 5 replicates each receiving ^{13}C-only labelled litter for harvest at 10, 21, 42, and 70 days, and 2 treatments with 5 each replicates receiving $^{13}C^{15}N$-labeled litter for harvest at 70 days.

To establish AMF colonization, two weeks prior to the start of the experiment, the planted chamber received 120 g fresh weight inoculum comprised of *G. hoi* colonized roots (*P. lanceolata*) in a sand and Terra-Green® growth medium (Oil-Dri, Cambridgeshire, UK). The inoculum was mixed thoroughly with 1.85 L of a 50:50 mix of sand:Terra-Green® and 0.3 g L^{-1} sterilized bone-meal. *P. lanceolata* seeds (Emorsgate Seeds, Norfolk, UK) were planted in this plant compartment (one seed per unit).

The litter chamber contained 2 mm sieved loam soil (pH 6.8 in 0.01 M $CaCl_2$) collected from an experimental garden at the University of York, UK. A PVC pipe was used to precisely add the isotopically labelled root litter two weeks after setup, while ensuring minimal disturbance to the

system (internal diameter 6.5 cm, depth 8 cm). The litter was added as 2 g of dried root material (*P. lanceolata*) either labelled with ^{13}C only or dual-labelled with ^{13}C and ^{15}N. Root litter was mixed with 60 g of loam soil prior to burial at 5 cm depth. All root litter was enriched to 40 ± 0.3 atom% ^{13}C. Dual-labeled root litter was enriched to 40 ± 0.3 atom% ^{13}C and 27 ± 0.6 atom% ^{15}N. Litter-soil zones were *c*. 1 cm in depth, 6.5 cm in diameter, had a bulk density of 1.9 mg m^{-3}, and were placed at a distance of 3 cm from the mesh to the litter-soil perimeter. Production and characteristics of the litter material is described in Herman *et al.* 2012.

The experiment was set-up in a randomized design in a glasshouse at the University of York, UK. The daily mean temperature during the experiment was 19.4 ^{o}C ± 0.07. Photosynthetically active radiation flux was recorded weekly at noon and averaged 190.5 ± 37.2 μmol m^{-2} s^{-1} at plant level. All compartments were watered daily with deionised water. The planted compartment was irrigated twice weekly with 50 mL nutrient solution (Leigh *et al.* 2009). The litter compartment received no additional nutrients.

Mycorrhizal Root Colonization Assessment. A subsample of living root material was used for mycorrhizal assessment and examined with a Nikon Optiphot-2 microscope using brightfield and epifluorescence settings at x 200 magnification (Leigh *et al.* 2009). Roots were washed and then stained with acid fuchsin to visualize the AMF colonization (Leigh *et al.* 2011). Numbers of arbuscules, vesicles, and total root length colonized (RLC; the percentage of total intercepts where hyphae or other AM fungal structures were present) were recorded for each intersection. A minimum of 100 intersections were checked for each sample.

Mycorrhizal Hyphal Length Assessment. AMF extraradical mycelium (ERM) were extracted from the litter-soil material using a modified membrane filter technique, stained with acid fuchsin, and counted with at least 50 fields of view at x 125 magnification using the gridline intercept method (Leigh *et al.* 2009). Hyphal lengths were then converted to hyphal length densities (m hyphae g^{-1} soil d. wt).

Soil DNA Extraction. Soil taken from the litter-soil material was frozen at -80 ^{o}C within an hour of harvest. The 42-day harvest was selected for analysis because the AMF were clearly present in the root litter-soil at this time point (Figures 1c and 1d), and had 5 replicates of each treatment (AMF Permitted vs. AMF Excluded). DNA was extracted in triplicate from 0.25 g aliquots of freeze-dried soil using the PowerSoil DNA Isolation Kit (MoBio Laboratories, Inc., Solana Beach CA), where samples were bead-beaten for 30 sec at 5.5m/s with FastPrep Instrument (Qbiogene, Inc., Irvine CA).

PCR Amplification of Target DNA. Bacterial and archaeal 16S rRNA genes were PCR amplified using the primers 1492rpl (universal reverse), 8F* (bacterial), and 4Fa (archaeal) (Wilson *et al.* 1990; Hershberger *et al.* 1996). PCR amplifications were performed as 8 replicates of 25 µl final volumes of 1x Takara buffer, 0.3 µM primers, 1.5U Takara ExTaq, 0.8 mM dNTP, and 20 µg BSA (Takara Mirus Bio Inc., Madison WI). 0.25 µl volumes of DNA extract were added as undiluted archaeal template or 1:10 diluted bacterial template. Templates were amplified in a BioRad myCycler (BioRad, Hercules CA) using the following conditions: 95°C (3 min), 25 cycles at 95°C (30 sec), 48-58°C gradient (25 sec), and 72°C (2 min), followed by 72°C (10 min). Bacterial PCR products were purified using the UltraClean PCR Clean-Up Kit (MoBio Laboratories, Inc., Solana Beach CA). Archaeal PCR products were gel purified

using the QiaQuick Gel Extraction Kit (Qiagen Sciences, Valencia CA). PCR products were electrophoresed on a 2% E-Gel (Invitrogen, Carlsbad CA) for 18 min and quantified using Quantity One 1-D analysis software (BioRad, Hercules CA). Purified PCR products were concentrated using microcon-30 centrifugal filters (Millipore, Billerica MA).

Microarray Analysis. For high-throughput identification of bacteria and archaea, 500 ng bacterial amplicons, 100 ng archaeal amplicons, and a known concentration of synthetic control DNA were fragmented, biotin-labeled, and hybridized to the Phylochip G2 microarray (Brodie *et al.* 2007). Chips were washed, scanned, and normalized using the same criteria as Brodie *et al*. 2007. An additional normalization was used to account for differences in chip brightness, where the intensity units for individual taxa were divided by the average probe brightness for all detected taxa. Taxa were identified using the 2010 *Greengenes* phylogeny. To qualify as present in the dataset, taxa were required to pass a probe quartile criteria (Hazen *et al.* 2010), have a probe fraction of 0.9 or higher, and be detected in a minimum of three microarray replicates for at least one treatment.

Microarray Statistical Analysis. Community structure was ordinated by nonmetric multidimensional scaling (NMDS) using the *vegan* R package (dissimilarity measure: Bray-Curtis) (Oksanen *et al.* 2010). Analysis of similarities (anosim) was used to evaluate the null hypothesis of no difference between groups (distance measure: Bray-Curtis). Operational taxonomic units (OTUs) that significantly differed between the treatments were determined using indicator species analysis (ISA) on relative abundance data (Dufrene & Legendre 1997). ISA determines which taxa are uniquely present for each treatment, and accounts for both the relative abundance and frequency of an OTU (Dufrene & Legendre 1997). Mean differences in

relative abundance (RA) between the two treatments were used to confirm whether taxa responded positively or negatively (increased or decreased) in the presence of AMF ($\Delta\overline{RA} = \overline{RA}_{AMF\ Permitted} - \overline{RA}_{AMF\ Excluded}$, n = 5).

Phylogenetic Dispersion Analysis. Net relatedness index (NRI) and nearest taxa index (NTI) analyses were used to determine if the subset of the community that responded to AMF was phylogenetically clustered or overdispersed (Webb *et al.* 2002). Phylogenetic dispersion was evaluated separately for the positive and negative AMF responders. NRI and NTI values were calculated as $NRI = SES_{MPD} \times -1$ and $NTI = SES_{MNTD} \times -1$ and weighted by relative abundance in the *picante* R package (Kembel *et al.* 2010). Significance was assigned to any NRI or NTI value falling in the top or bottom 2.5% of randomized communities created using the independent swap null model (10,000 randomizations, each with 10,000 swaps). NRI values significantly > 0 indicate clustering within deeper branches of the tree, while NTI values significantly > 0 indicate clustering at the terminal branches of the tree. NRI and NTI values significantly < 0 indicate that the traits are evenly dispersed on the tree (overdispered), while values that are indistinguishable from 0 indicate random dispersal on the tree. The independent swap null model maintains species occurrence frequency and species richness, and this null model performs well when detecting niche-based assembly processes compared to other null models (Kembel 2009). The phylogenetic tree used for NRI and NTI analysis was constructed from all bacterial taxa detected in this study. The sequences corresponding to the probe sets were compiled and aligned using *Greengenes* (DeSantis *et al.* 2006). The maximum likelihood tree was created in *FastTree* using the generalized time reversible model and the gamma setting to optimize branch lengths (Price *et al.* 2010). A smaller maximum likelihood tree was generated using the same conditions to display the subset of the bacteria that responded to AMF (Figure 3).

IRMS analysis. Carbon and nitrogen content and isotope ratios were analysed at 42 and 70 days using a Roboprep automated nitrogen-carbon analyzer coupled to a model 20-20 isotope ratio mass spectrometer (IRMS) (Sercon, Ltd., Crewe, Cheshire, UK) (Herman *et al.* 2012). To determine the percent litter-^{15}N that was in the plant shoots, roots, microbial biomass, or remained in the litter-soil material, the ^{15}N in each component at day 70 was divided by the initial litter ^{15}N added to the soil: $\%^{15}N_{Derived\ from\ Litter} = \frac{^{15}N_{Component_f}\ (mg)}{^{15}N_{Litter_i}\ (mg)}$.

NanoSIMS Analysis. NanoSIMS analyses were performed to localize and quantify ^{15}N/^{14}N and ^{13}C/^{12}C ratios in *P. lanceolata* roots and associated colonizing AMF using the Lawrence Livermore National Laboratory NanoSIMS 50 (Gennevilliers, France). Samples from the 70-day dual-label treatment were prepared by transferring the slides prepared for the root length colonization (RLC) assessment to the surface of a 7 x 7 mm silica wafer and coating with 10 nm Au to ensure conductivity and prevent charging. Hyphae-colonized roots were imaged for ^{15}N/^{14}N and ^{13}C/^{12}C ratios with 5-15 contiguous analyses at each of 3 random locations using previously reported methods (Finzi-Hart *et al.* 2009). Individual images averaged 30 x 30 µm, and the areas were sputtered to a depth of 100 – 200 nm before 50 serial quantitative secondary ion images (i.e. layers) were collected. Data were processed and standardized as previously reported (Finzi-Hart *et al.* 2009). For each image, isotopic data were extracted for hyphae and roots separately using secondary electron images as a guide to morphology. Replicate measurements at greater depth at selected locations were used to ensure measurement accuracy.

RESULTS

We characterized the bacterial and archaeal communities in the litter-soil material after the AMF had colonized the decomposing litter. By 42 days, AM hyphae were clearly detectable in the decomposing litter (1.02 ± 0.13 SE m hyphae g^{-1} dry weight soil) (Figure 1c, 1d), while virtually no AM hyphae were detected in the exclusion controls at any time point (Figure 1d). When the AMF had access to the decomposing litter, the hyphae in the planted chamber on average colonized 2.1 times more root material and produced 4 times more arbuscules by 70 days (Two-way ANOVA: $F_{3, 32} = 17.82$, $p < 0.001$) (Supplemental Figures 1a, 1b).

We detected a total of 3791 taxa in the litter-soil material using 16S rRNA gene-based microarray analysis (see methods for presence – absence criteria). We detected 3535 ± 54 OTUs in the litter-soil where AMF was permitted (n = 5), and 3632 ± 79 OTUs in the exclusion controls (n = 5). Approximately 10.1% (384) of the taxa significantly increased or decreased in response to AMF based on indicator species analysis (ISA: n = 5, $p < 0.05$).

The taxa that responded to AMF clustered by treatment in NMDS ordination space (Figure 2) (anosim: R = 0.644, p = 0.008). Litter colonized by the AMF had a higher relative abundance of Firmicutes, Gemmatimonadetes, Deltaproteobacteria, and Planctomycetes (Figure 3). Within the Firmicutes, the taxa that increased in relative abundance were within the subphyla Bacilli, Clostridia, Alicyclobacillus, and Mollicutes, among others (Table 1). We used NRI and NTI to assess if the taxa that responded to AMF had significant phylogenetic patterns. Bacterial taxa that responded positively to the presence of AMF in the decomposing litter were significantly clustered within the deeper branches of the soil phylogenetic tree (NRI: 2.37 ± 0.13, p = 0.014), but were overdispersed at the terminal branches of the tree (NTI: -3.01 ± 0.03, $p < 0.001$).

The bacteria that responded negatively to the presence of AMF showed significant phylogenetic clustering both basally and at the terminal leaves of the phylogenetic tree (NRI: 2.52 ± 0.05, $p = 0.007$; NTI: 7.66 ± 0.10, $p < 0.001$). Relative to the control, the AMF treatment had a lower relative abundance of Betaproteobacteria, Actinobacteria, and Bacteriodetes (Figure 3). Within the Betaproteobacteria, the Comamonadaceae had the most taxa that declined in relative abundance (32 taxa) (Supplemental Table 1). In the Actinobacteria, the taxa that decreased in relative abundance were from the orders Streptosporangineae and Propionibacterineae (17 and 10 taxa, respectively). Finally, within Bacteriodetes, the Bacteroidales and Flavobacteriales had the most taxa decrease in relative abundance (10 and 8 taxa, respectively). Only one archaeon (family Methanosarcinaceae) significantly responded to the presence of AMF, and it had a negative response.

Because of the intimate nature of AMF-root colonization, it can be difficult to differentiate the ^{15}N-enrichment of the AM hyphae from that of the associated root tissue using standard IRMS analysis; hence we used NanoSIMS to distinguish the enrichment of these two tissue types. At the final harvest (70 days), NanoSIMS analyses of multiple AM-colonized live roots showed that the hyphae associated with living roots in the planted chamber were significantly enriched in ^{15}N, demonstrating that the hyphae exported litter-^{15}N from the litter chamber to the plant roots (Figure 4a). The average ^{15}N enrichment of the hyphae from the NanoSIMS analysis was 24000‰ ± 1400 ^{15}N ($n = 28$), which was significantly higher than that of the associated roots, which were enriched at 2800‰ ± 600 ^{15}N ($n = 53$). NanoSIMS analyses also showed a slight enrichment of litter-^{13}C in the individual hyphae (68‰ ±13 ^{13}C) compared to adjacent plant roots (-50‰ ± 4 ^{13}C), though with substantial spatial heterogeneity along the length of the hyphal

sections analyzed (Figure 4b). By the end of the experiment, IRMS analysis determined that AM hyphae had exported 4.89% ± 0.33 of the litter-^{15}N to the host plant, whereas the plants whose AM fungal partner was excluded from the litter acquired only 0.05% ± 0.06 of the litter-^{15}N through mass flow (Table 2). The shoots acquired significantly more of the litter-^{15}N than the roots, indicating that the enrichment in the plant was not simply due to the hyphae associated with the plant roots (Table 2).

In the litter chamber, we determined that the presence of AMF increased the ^{13}C:^{15}N ratio of the litter-soil. This indicates that proportionally more ^{15}N had been removed from the litter-soil than ^{13}C (Table 2). While there is a trend toward decreased ^{15}N in the litter-soil, the two treatments were not statistically distinguishable (Table 2). We also did not see a difference in C content or ^{13}C isotopic enrichment between the two treatments (data not shown). Approximately 38.5% of the litter ^{15}N remained in the original location of the litter-soil material at the end of the experiment, while an additional 5.7% remained in the soil microbial biomass.

DISCUSSION

Previous studies show that AMF alter the decomposition rate of organic material, but the mechanisms by which AMF modify decomposition are not understood (Hodge *et al.* 2001; Hodge & Fitter 2010). We demonstrate that the AMF *G. hoi* significantly altered approximately 10% of the soil bacterial community inhabiting decomposing litter (Hypothesis 1). Interestingly, the taxa that responded to AMF were structured phylogenetically, which suggests that AMF may have a role in bacterial community assembly in decomposing litter. To our knowledge, this is the first study to examine the bacterial and archaeal communities associated with AMF using molecular tools that have high phylogenetic resolution. In addition, we show that AMF alter the physicochemical environment of decomposing litter by exporting N (Hypothesis 2). NanoSIMS provides the first isotopic images of AMF associated with root tissues by mapping the ^{15}N and ^{13}C that was exported from the decomposing litter to the host plant.

Based on previous results from litter decomposition studies (el Zahar Haichar *et al.* 2007; Lee *et al.* 2011), we expected that members of the phyla Actinobacteria, Firmicutes, and Bacteroidetes would be stimulated when the AMF were allowed to access the decomposing litter. We found that taxa within the phylum Firmicutes (Clostridia and Bacilli) tended to increase in relative abundance in the presence of AMF, while taxa within the phyla Actinobacteria and Bacteroidetes generally decreased in the presence of AMF (Figure 3). It appears that the AMF shifted the relative abundances of the decomposer community from the phyla Actinobacteria and Bacteroidetes to the phylum Firmicutes. Many members of the bacterial class Clostridia are known to produce multienzyme cellulosome complexes, which are capable of catalyzing the efficient degradation of cellulose (Bayer *et al.* 1998). Previous work has shown that Bacilli associate with AMF (Andrade *et al.* 1997), and in particular with decomposing hyphae

(Artursson & Jansson 2003; Toljander *et al.* 2007). Our finding that Actinobacterial taxa predominantly decreased in relative abundance was unexpected, given that some strains of Actinobacteria have been shown to have a beneficial impact on AMF hyphal growth and root colonization (Franco-Correa *et al.* 2010). Actinobacteria are renowned for producing a wide variety of secondary metabolites and antibiotics (Bérdy 2005). Altering the composition of Actinobacteria could modify the suite of bioactive compounds in the soil, and provide either an advantageous or an inhospitable environment to neighboring fungi or bacteria.

A striking result from this study was the decrease of Proteobacteria in response to AMF, particularly within the Beta-Proteobacterial family Comamonadaceae. The Comamonadaceae are a physiologically heterogeneous group of bacteria; they are known to consume a broad spectrum of organic carbon compounds that range from simple sugars to complex aromatic compounds, as well as assimilate inorganic carbon autotrophically (Kersters *et al.* 2006). In the *Medicago truncatula* rhizosphere, the presence of AMF increased the relative abundance of Comamonadaceae taxa (Offre *et al.* 2007). However, further study found that Comamonadaceae strains isolated from the *Medicago* rhizosphere had no effect on or decreased root colonization, and in one case depressed AMF spore germination and hyphal proliferation (Pivato *et al.* 2009). We found that 32 taxa from the Comamonadaceae decreased in relative abundance in decomposing litter in the presence of AMF, while only one taxa increased in relative abundance. This indicates that the many members of the Comamonadaceae are repressed by the presence of AMF in decomposing litter. While AMF are not known to produce antibiotics, the presence of AMF has been shown to repress some members of the microbial community (Green *et al.* 1999; Welc *et al.* 2010), including fungal pathogens (Filion *et al.* 1999). The mechanisms for these interactions are unknown, and may result from the direct or indirect manipulation of the

community through hyphal exudates (Toljander *et al.* 2007), or the AMF may occupy the same niche as these microbes and outcompete them for the acquisition of nutrients.

It is well known that AMF can transport P to the host plant, which may constitute a loss for the soil microbial community surrounding the extraradical hyphae (Smith & Smith 2011). As our work and the recent literature shows, it is becoming more apparent that AMF can perform a similar process with N (Hodge & Fitter 2010). AMF competition for N would likely have a significant effect on the microbial community, as the scarcity of N limits productivity in most temperate soils (Vitousek & Howarth 1991). In our work, the AM fungi exported a substantial portion of the litter ^{15}N, with approximately 5% of the litter ^{15}N appearing in the host plant. Our detection of this effect in live soil confirms that this AMF is capable of drawing significant amounts of N away from decomposing litter, even when the AM hyphae are competing for N acquisition with a diverse and populous soil microbial community. While recent work has suggested that AMF can uptake N as simple amino acids (Hawkins *et al.* 2000; Whiteside *et al.* 2009), or even as the complex N macromolecule chitosan (Whiteside *et al.* 2009), we did not see evidence for organic N uptake in our study. The amount of ^{13}C enrichment detected in the AMF associated with roots was far less than the ^{15}N enrichment in the same hyphae (68‰ ^{13}C vs. 24000‰ ^{15}N), suggesting that the AMF did not acquire C through active decomposition, but instead relied on the surrounding microbial community to decompose the litter and make inorganic N available to the AMF. The trace levels of ^{13}C enrichment we detected in the hyphae were likely due to a small amount of C fixation by the fungus through gluconeogenesis (Pfeffer *et al.* 2004), though it is possible that amino acids were taken up in very small amounts.

We also observed that the presence of AMF significantly increased the ^{13}C:^{15}N ratio in the litter-soil, indicating that the presence of AMF increased the C:N content of the remaining litter. During decomposition, the C:N ratio of litter usually declines due to the loss of C as CO_2. In numerous studies, the rate of litter decomposition has been shown to be a function of N availability, where lower N concentrations stimulate decomposition (Knorr *et al.* 2005). Though our experimental design did not allow us to directly quantify the rate of litter decomposition, accelerated litter decomposition in the presence of AMF has been reported (Hodge *et al.* 2001; Atul-Nayyar *et al.* 2009). We hypothesize that the preferential export of N is one mechanism by which AMF alter the microbial community in decomposing litter, as well as decomposition rates.

Finally, we observed that the AMF-responsive taxa were more phylogenetically structured than expected by chance using the phylogenetic dispersion metrics NRI and NTI. NRI provides an index of basal clustering of taxa on a phylogenetic tree, while NTI assesses local clustering at the terminal branches of the phylogenetic tree, independent of deeper clustering (Webb *et al.* 2002). Patterns of clustering and overdispersion can both indicate phenotypic attraction among taxa, such as when traits have been conserved among closely related taxa (clustered), or when distantly related taxa have converged upon similar niche use (overdispersed) (Webb *et al.* 2002). Phenotypic attraction was indicated for the taxa that responded to AMF; the taxa that responded positively were clustered basally and were overdispersed at the terminal branches of the tree, while the taxa that responded negatively clustered basally and strongly clustered at the terminal branches of the tree. Since bacteria are highly diverse, interact at microscopic spatial scales, and have undergone billions of years of evolution, it is difficult to invoke a single mechanism of community assembly to explain phenotypic attraction in bacterial communities (Vamosi *et al.* 2009). We posit that one way AMF drive phenotypic attraction is by acting as a habitat filter. As

shown in this study, AMF modify the physicochemical environment of the soil by exporting litter-N, which increases the litter-C:N locally in the soil. In addition, AMF export P to the plant (Smith & Smith 2011), and import photosynthate C from distant roots (Herman *et al.* 2012). The removal of the P and inorganic N by AMF could deplete the local environment of readily accessible forms of nutrients, and instigate inter-domain competition between the bacterial community and AMF (Leigh *et al.* 2011; Smith & Smith 2011). Additional mechanisms that may drive phenotypic attraction are mutualisms that have developed between the AMF and the microbial community, such as endosymbioses (Naumann *et al.* 2010), or the facilitation of bacterial populations by imported C (Toljander *et al.* 2007).

We demonstrated that the AMF *G.hoi* significantly altered the bacterial community in decomposing litter and that the responding taxa were structured phylogenetically, which suggests that AMF may have a role in microbial community assembly. We also demonstrated that AMF modified the physicochemical environment in the decomposing litter by preferentially exporting N. Our analysis suggests that AMF took up N in the mineral form, which indicates that the fungus relied on the surrounding microbial community for litter decomposition and N-mineralization. We propose that the export of N from litter is one mechanism by which AMF alter the composition of bacteria in the decomposing litter. The localized reduction of N in decomposing litter is likely to alter litter decomposition rates. As the AMF-plant symbiosis is ubiquitous in terrestrial ecosystems, the influence of AMF on decomposition is broadly relevant across terrestrial ecosystems for the utilization and ultimate stabilization of plant carbon.

ACKNOWLEDGEMENTS

This work was funded by an Underwood Fellowship (BBSRC) and California Experiment Station project 6117-H to MKF, research grant BB/E016359/1 (BBSRC) to AH, and the US DOE Genomics Science program and LLNL LDRD program (10-ERD-021). We thank Alastair Fitter, Eoin Brodie, Todd DeSantis, Yvette Piceno, Rebecca Daly, David Armitage, Jeremy Bougoure for valuable advice or technical assistance. NanoSIMS analyses were performed under the auspices of the US DOE at LLNL (DE-AC52-07NA27344).

REFERENCES

Andrade G., Mihara K.L., Linderman R.G. & Bethlenfalvay G.J. (1997). Bacteria from rhizosphere and hyphosphere soils of different arbuscular-mycorrhizal fungi. *Plant and Soil*, 192, 71-79.

Artursson V. & Jansson J.K. (2003). Use of bromodeoxyuridine immunocapture to identify active bacteria associated with arbuscular mycorrhizal hyphae. *Applied and Environmental Microbiology*, 69, 6208-6215.

Atul-Nayyar A., Hamel C., Hanson K. & Germida J. (2009). The arbuscular mycorrhizal symbiosis links N mineralization to plant demand. *Mycorrhiza*, 19, 239-246.

Bayer E.A., Shimon L.J.W., Shoham Y. & Lamed R. (1998). Cellulosomes—Structure and Ultrastructure. *Journal of Structural Biology*, 124, 221-234.

Bérdy J. (2005). Bioactive Microbial Metabolites. *The Journal of Antibiotics*, 58, 1-26.

Brodie E.L., DeSantis T.Z., Parker J.P.M., Zubietta I.X., Piceno Y.M. & Andersen G.L. (2007). Urban aerosols harbor diverse and dynamic bacterial populations. *Proceedings of the National Academy of Sciences*, 104, 299-304.

Brundrett M. (2002). Coevolution of roots and mycorrhizas of land plants. *New Phytologist*, 154, 275-304.

DeSantis T.Z., Hugenholtz P., Keller K., Brodie E.L., Larsen N., Piceno Y.M., Phan R. & Andersen G.L. (2006). NAST: a multiple sequence alignment server for comparative analysis of 16S rRNA genes. *Nucleic Acids Research*, 34, W394-W399.

Dufrene M. & Legendre P. (1997). Species assemblages and indicator species: The need for a flexible asymmetrical approach. *Ecological Monographs*, 67, 345-366.

el Zahar Haichar F., Achouak W. & Christen R. (2007). Identification of cellulolytic bacteria in soil by stable isotope probing. *Environmental Microbiology*, 9, 625-634.

Filion M., St-Arnaud M. & Fortin J.A. (1999). Direct interaction between the arbuscular mycorrhizal fungus Glomus intraradices and different rhizosphere microorganisms. *New Phytologist*, 141, 525-533.

Finzi-Hart J.A., Pett-Ridge J., Weber P.K., Popa R., Fallon S.J., Gunderson T., Hutcheon I.D., Nealson K.H. & Capone D.G. (2009). Fixation and fate of C and N in the cyanobacterium *Trichodesmium* using nanometer-scale secondary ion mass spectrometry. *Proceedings of the National Academy of Sciences*, 106, 6345-6350.

Franco-Correa M., Quintana A., Duque C., Suarez C., Rodriguez M.X. & Barea J.-M. (2010). Evaluation of actinomycete strains for key traits related with plant growth promotion and mycorrhiza helping activities. *Applied Soil Ecology*, 45, 209-217.

Frey-Klett P., Garbaye J. & Tarkka M. (2007). The mycorrhiza helper bacteria revisited. *New Phytologist*, 176, 22-36.

Green H., Larsen J., Olsson P., Jensen D. & Jakobsen I. (1999). Suppression of the biocontrol agent *Trichoderma harzianum* by mycelium of the arbuscular mycorrhizal fungus *Glomus intraradices* in root-free soil. *Applied and Environmental Microbiology*, 65, 1428-1434.

Hawkins H., Johansen A. & George E. (2000). Uptake and transport of organic and inorganic nitrogen by arbuscular mycorrhizal fungi. *Plant and Soil*, 226, 275-285.

Hazen T.C., Dubinsky E.A., DeSantis T.Z., Andersen G.L., Piceno Y.M., Singh N., Jansson J.K., Probst A., Borglin S.E., Fortney J.L., Stringfellow W.T., Bill M., Conrad M.E., Tom L.M., Chavarria K.L., Alusi T.R., Lamendella R., Joyner D.C., Spier C., Baelum J., Auer M., Zemla M.L., Chakraborty R., Sonnenthal E.L., D'haeseleer P., Holman

H.Y.N., Osman S., Lu Z., Van Nostrand J.D., Deng Y., Zhou J. & Mason O.U. (2010). Deep-Sea Oil Plume Enriches Indigenous Oil-Degrading Bacteria. *Science*, 330, 204-208.
Herman D.J., Firestone M.K., Nuccio E., Pett-Ridge J. & Hodge A. (2012). Interactions between an arbuscular mycorrhizal fungus and a soil microbial community mediating litter decomposition. *FEMS Microbiology Ecology*, (Online Early).
Hershberger K., Barns S., Reysenbach A., Dawson S. & Pace N. (1996). Wide diversity of Crenarchaeota. *Nature*, 384, 420-420.
Hodge A., Campbell C.D. & Fitter A.H. (2001). An arbuscular mycorrhizal fungus accelerates decomposition and acquires nitrogen directly from organic material. *Nature*, 413, 297-299.
Hodge A. & Fitter A.H. (2010). Substantial nitrogen acquisition by arbuscular mycorrhizal fungi from organic material has implications for N cycling. *Proceedings of the National Academy of Sciences*, 107, 13754-13759.
Johnson D., Leake J., Ostle N., Ineson P. & Read D. (2002). In situ 13CO2 pulse-labelling of upland grassland demonstrates a rapid pathway of carbon flux from arbuscular mycorrhizal mycelia to the soil. *New Phytologist*, 153, 327-334.
Kembel S.W. (2009). Disentangling niche and neutral influences on community assembly: assessing the performance of community phylogenetic structure tests. *Ecology Letters*, 12, 949-960.
Kembel S.W., Cowan P.D., Helmus M.R., Cornwell W.K., Morlon H., Ackerly D.D., Blomberg S.P. & Webb C.O. (2010). Picante: R tools for integrating phylogenies and ecology. *Bioinformatics*, 26, 1463-1464.
Kersters K., Vos P., Gillis M., Swings J., Vandamme P. & Stackebrandt E. (2006). Introduction to the Proteobacteria. In: *The Prokaryotes* (ed. Dworkin M). Springer New York, pp. 3-37.
Knorr M., Frey S. & Curtis P. (2005). Nitrogen additions and litter decomposition: A meta-analysis. *Ecology*, 86, 3252-3257.
Lee C.G., Watanabe T., Sato Y., Murase J., Asakawa S. & Kimura M. (2011). Bacterial populations assimilating carbon from 13C-labeled plant residue in soil: Analysis by a DNA-SIP approach. *Soil Biology and Biochemistry*, 43, 814-822.
Leigh J., Fitter A.H. & Hodge A. (2011). Growth and symbiotic effectiveness of an arbuscular mycorrhizal fungus in organic matter in competition with soil bacteria. *FEMS Microbiology Ecology*, 76, 428-438.
Leigh J., Hodge A. & Fitter A.H. (2009). Arbuscular mycorrhizal fungi can transfer substantial amounts of nitrogen to their host plant from organic material. *New Phytologist*, 181, 199-207.
Naumann M., Schüssler A. & Bonfante P. (2010). The obligate endobacteria of arbuscular mycorrhizal fungi are ancient heritable components related to the *Mollicutes*. *ISME Journal*, 4, 862-871.
Nicolson T.H. (1959). Mycorrhiza in the Gramineae: I. Vesicular-arbuscular endophytes, with special reference to the external phase. *Transactions of the British Mycological Society*, 42, 421-438.
Offre P., Pivato B., Siblot S., Gamalero E., Corberand T., Lemanceau P. & Mougel C. (2007). Identification of bacterial groups preferentially associated with mycorrhizal roots of *Medicago truncatula*. *Applied and Environmental Microbiology*, 73, 913-921.
Oksanen J., Blanchet F.G., Kindt R., Legendre P., O'Hara R., Simpson G.L., Solymos P., Stevens H.H. & Wagner H. (2010). Vegan: Community Ecology Package. http://CRAN.R-project.org/package=vegan.

Parniske M. (2008). Arbuscular mycorrhiza: the mother of plant root endosymbioses. *Nature Reviews Microbiology*, 6, 763-75.
Pfeffer P., Douds Jr D., Bücking H., Schwartz D. & Shachar□Hill Y. (2004). The fungus does not transfer carbon to or between roots in an arbuscular mycorrhizal symbiosis. *New Phytologist*, 163, 617-627.
Pivato B., Offre P., Marchelli S., Barbonaglia B., Mougel C., Lemanceau P. & Berta G. (2009). Bacterial effects on arbuscular mycorrhizal fungi and mycorrhiza development as influenced by the bacteria, fungi, and host plant. *Mycorrhiza*, 19, 81-90.
Price M.N., Dehal P.S. & Arkin A.P. (2010). FastTree 2 - Approximately maximum-likelihood trees for large alignments. *PLoS ONE*, 5, e9490.
Remy W., Taylor T.N., Hass H. & Kerp H. (1994). Four hundred-million-year-old vesicular arbuscular mycorrhizae. *Proceedings of the National Academy of Sciences*, 91, 11841-11843.
Scheublin T.R., Sanders I.R., Keel C. & van der Meer J.R. (2010). Characterisation of microbial communities colonising the hyphal surfaces of arbuscular mycorrhizal fungi. *ISME Journal*, 4, 752-763.
Schmidt M.W.I., Torn M.S., Abiven S., Dittmar T., Guggenberger G., Janssens I.A., Kleber M., Kögel-Knabner I., Lehmann J., Manning D.A.C., Nannipieri P., Rasse D.P., Weiner S. & Trumbore S.E. (2011). Persistence of soil organic matter as an ecosystem property. *Nature*, 478, 49-56.
Smith S.E. & Smith F.A. (2011). Roles of arbuscular mycorrhizas in plant nutrition and growth: New paradigms from cellular to ecosystem scales. *Annual Review of Plant Biology*, 62, 227-250.
St. John T.V., Coleman D.C. & Reid C.P.P. (1983). Association of vesicular-arbuscular mycorrhizal hyphae with soil organic particles. *Ecology*, 64, 957-959.
Staddon P.L., Ramsey C.B., Ostle N., Ineson P. & Fitter A.H. (2003). Rapid turnover of hyphae of mycorrhizal fungi determined by AMS microanalysis of C-14. *Science*, 300, 1138-1140.
Toljander J.F., Lindahl B.D., Paul L.R., Elfstrand M. & Finlay R.D. (2007). Influence of arbuscular mycorrhizal mycelial exudates on soil bacterial growth and community structure. *FEMS Microbiology Ecology*, 61, 295-304.
Vamosi S.M., Heard S.B., Vamosi J.C. & Webb C.O. (2009). Emerging patterns in the comparative analysis of phylogenetic community structure. *Molecular Ecology*, 18, 572-592.
Vitousek P.M. & Howarth R.W. (1991). Nitrogen limitation on land and in the sea: how can it occur? *Biogeochemistry*, 13, 87-115.
Webb C., Ackerly D., McPeek M. & Donoghue M. (2002). Phylogenies and community ecology. *Annual Review of Ecology and Systematics*, 33, 475-505.
Welc M., Ravnskov S., Kieliszewska-Rokicka B. & Larsen J. (2010). Suppression of other soil microorganisms by mycelium of arbuscular mycorrhizal fungi in root-free soil. *Soil Biology & Biochemistry*, 42, 1534-1540.
Whiteside M.D., Treseder K.K. & Atsatt P.R. (2009). The brighter side of soils: Quantum dots track organic nitrogen through fungi and plants. *Ecology*, 90, 100-108.
Wilson K.H., Blitchington R.B. & Greene R.C. (1990). Amplification of bacterial 16S ribosomal DNA with polymerase chain reaction. *Journal of Clinical Microbiology*, 28, 1942-1946.

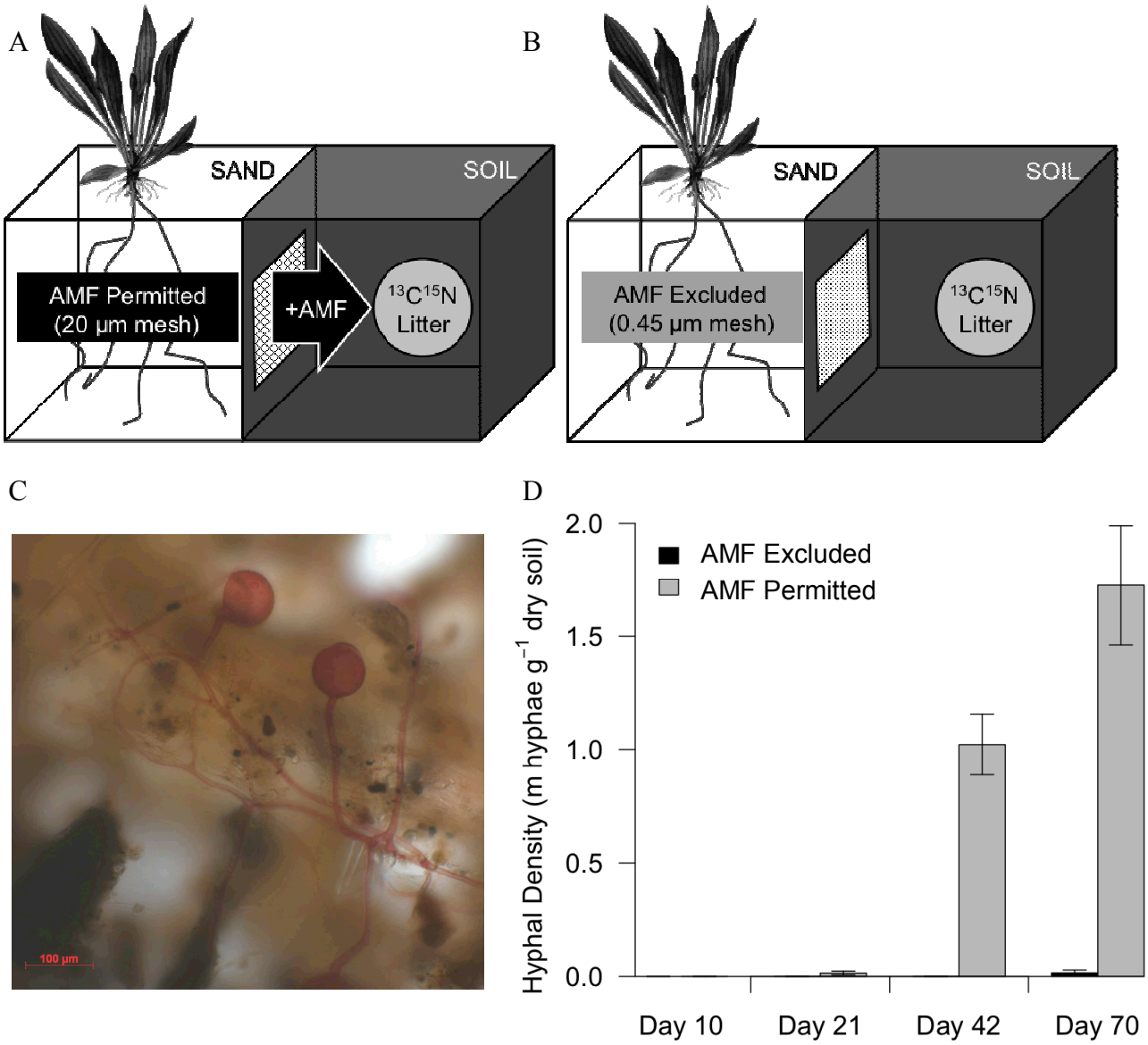

Figure 1: Dual-chamber experimental design. Planted chambers contain *Plantago lanceolata* L. and the arbuscular mycorrhizal fungus (AMF) *Glomus hoi* in a sand media, while litter chambers contain living soil and a region of ^{13}C or ^{13}C and ^{15}N dual-labeled root litter mixed with soil. The AMF Permitted treatment (A) has a 20 µm mesh separating the two chambers, which allows AMF to access the litter chamber, but excludes plant roots. The AMF Excluded treatment (B) has a 0.45 µm mesh separating the two chambers, which excludes both AMF and roots from the litter chamber, but allows solute diffusion between the chambers. (C) AMF arbuscules growing in the decomposing litter imaged by light microscopy at 42 days. (D) Hyphal length measurements in the litter chamber monitored over 70 days in soil where AMF is permitted or excluded from the decomposing litter (m hyphae g^{-1} dry soil).

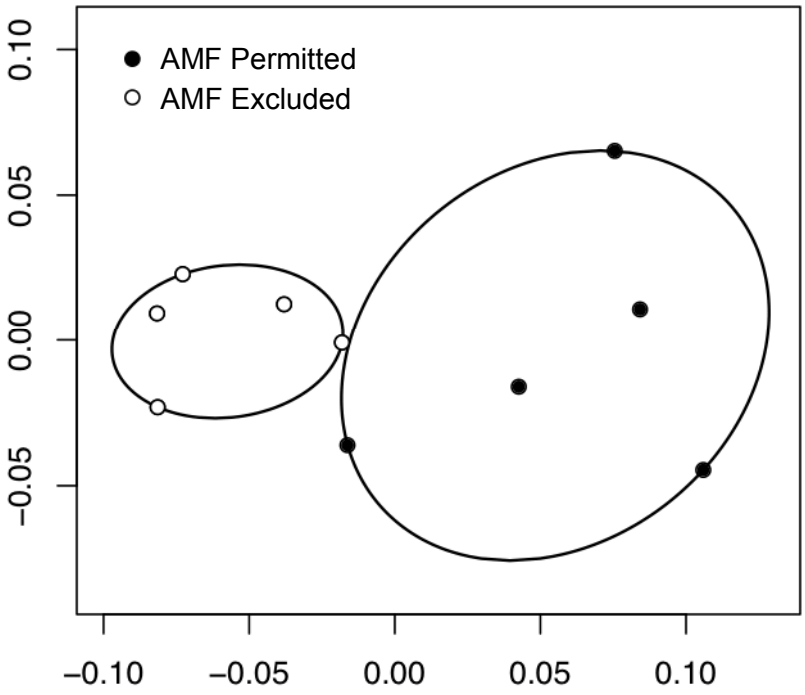

Figure 2: The effect of AMF on soil bacterial communities in decomposing litter after 42 days (NMDS ordination: Stress = 3.23%). Filled circles are units where AMF were permitted access to the litter chamber, and open symbols represent units where AMF were excluded. The ordination was completed on the operational taxonomic units (OTUs) identified by microarray analysis that significantly responded to the presence of AMF. The two treatments are distinguishable by anosim analysis (anosim: $R = 0.644$, $p = 0.008$).

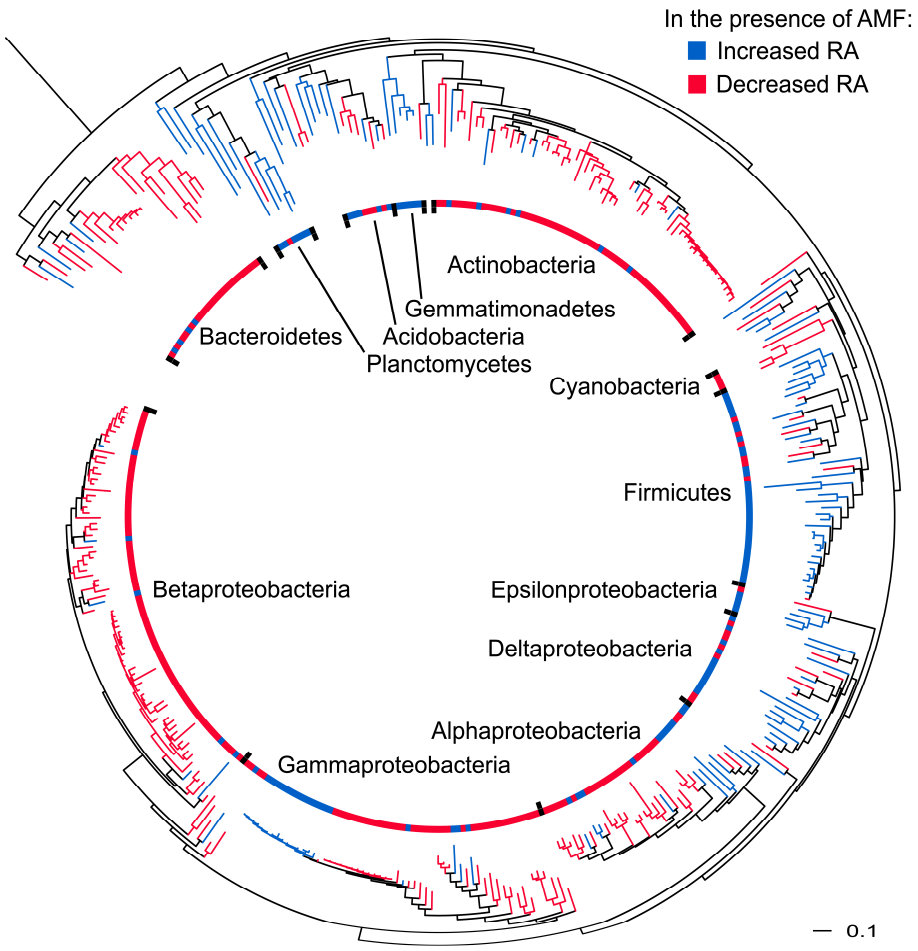

Figure 3: Maximum likelihood tree displaying the subset of bacteria that significantly increased (blue) or decreased (red) in relative abundance (RA) in the presence of AMF. Labels indicate the phyla of the branches, or subphyla for the Proteobacteria. The outgroup is the single Archaeal member of the dynamic subset, which is from the subphylum Methanosarcinales. The scale bar indicates the number of nucleotide substitutions per site.

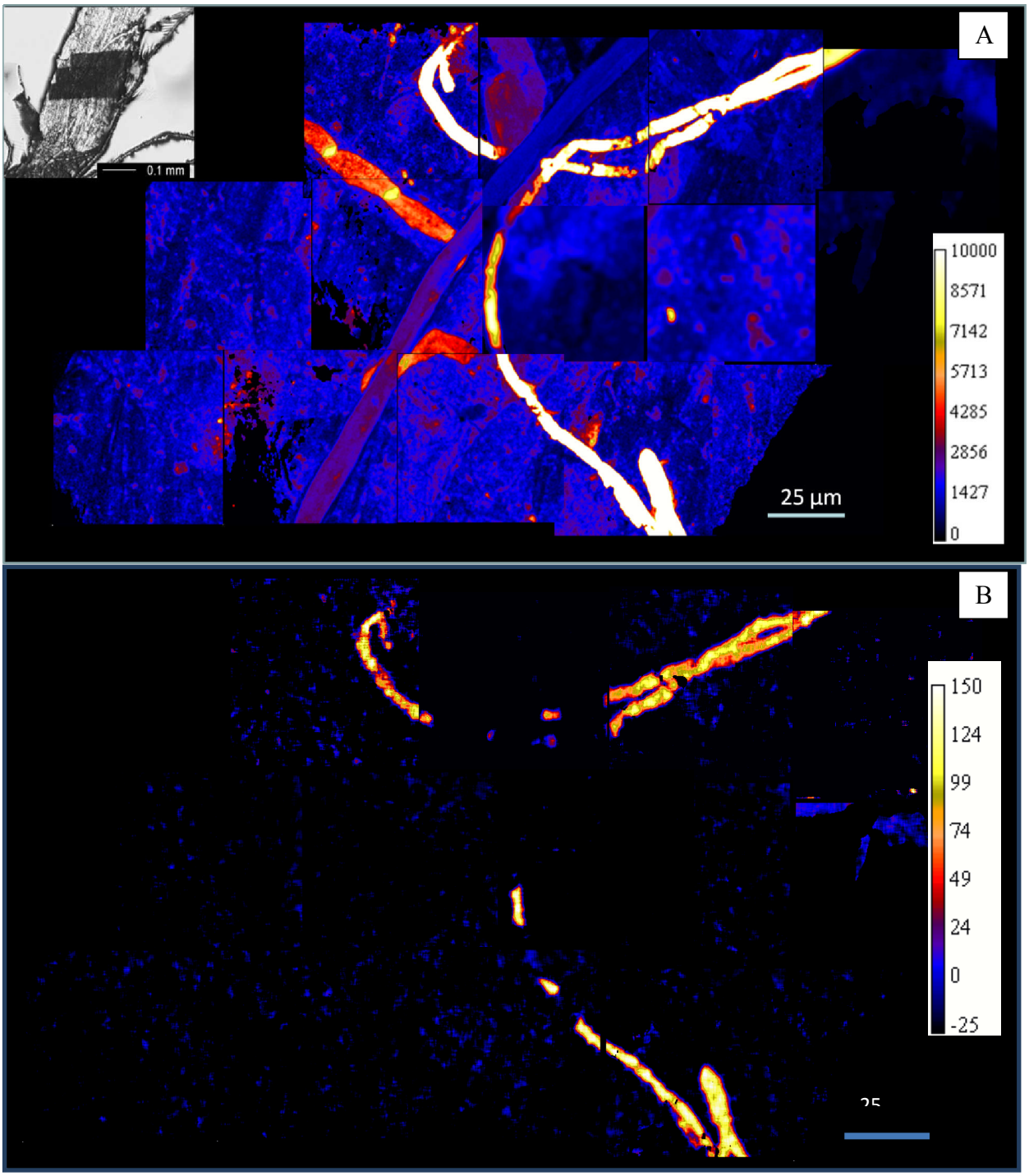

Figure 4. Composite of 14 NanoSIMS images of a *P. lanceolata* root colonized by *G. hoi* hyphae. Color scale bar represents (A) $\delta^{15}N$ enrichment and (B) $\delta^{13}C$ enrichment ranging from natural abundance (black) to 10,000+‰ (^{15}N) or 150‰ (^{13}C). Black and white inset image in (A) is a secondary electron micrograph taken post analysis, indicating the position of the NanoSIMS rasters as they transected the width of the colonized root.

Phylum	Subphylum	(+RA)	(-RA)
Methanomicrobia (A)	Methanosarcinales	0	1
AC1	Unclassified	1	0
Acidobacteria	Acidobacteriae	0	3
	iii1-15	1	0
	iii1-8	1	0
	RB25	1	0
	Solibacteres	2	2
Actinobacteria	Acidimicrobidae	1	3
	Actinobacteridae	5	49
	Coriobacteridae	0	1
	WCHB1-81	0	1
Bacteroidetes	Bacteroidales	0	7
	Flavobacteriales	1	8
	Flexibacterales	1	2
	Hymenobacterales	0	1
	LD1	0	1
	p-184-o5	0	3
	Pochenobacter	1	0
	Saprospirales	1	1
Chlorobi	BSV19	1	0
	OPB56	1	0
Chloroflexi	Anaerolineae	1	1
	Chloroflexi-4	0	1
	Dehalococcoidetes	2	0
Cyanobacteria	Nostoc	0	1
	Stigonematales	0	1
	Unclassified	0	1
Deferribacteres	Deferribacter	1	0
Firmicutes	Acidaminococcaceae	1	0
	Alicyclobacillus	2	0
	Bacilli	15	1
	Clostridia	12	5
	Desulfotomaculum	1	0
Firmicutes (cont.)	Mollicutes	2	0
	Unclassified	0	1
Gemmatimonadetes	Gemm-4	1	0
	Gemm-1b	3	0
	Gemm-5	1	0
	Gemmatibacter	1	0
Haloanaerobiales	Halanaerobiaceae	0	1
Marine_group_A	Unclassified	0	1
Nitrospirae	Thermodesulfovibrionales	1	0
OP3	PBS-25	1	0
OP8	OP8-1	1	0
Planctomycetes	Planctomycetacia	4	1
	Unclassified	1	0
	WPS-1	1	0
Proteobacteria	Alphaproteobacteria	11	25
	Betaproteobacteria	5	71
	Deltaproteobacteria	12	7
	Desulfovibrionales	1	0
	Epsilonproteobacteria	4	1
	Gammaproteobacteria	21	45
Spirochaetes	Leptospirales	1	0
	Spirochaetales	1	0
Synergistetes	Synergistes	0	1
	Thermovirga	1	0
	Unclassified	1	0
TM7	TM7-3	1	0
Unclassified	Unclassified	1	0
Verrucomicrobia	Opitutae	0	2
WCHB1-27	Unclassified	1	0
WPS-2	Unclassified	1	0
ZB3	Unclassified	1	0
Unclassified	Unclassified	1	0
Total		**134**	**250**

Table 1: Richness of the bacteria and archaea that significantly increased or decreased in relative abundance (RA) in response to AMF. An increase or decrease in relative abundance was calculated by subtracting the average of the normalized hybridization intensity of the AMF Permitted data from the AMF Excluded data. Significance was determined by indicator species analysis (ISA). The single archaeal taxon in the dynamic subset is denoted by (A).

Table 2: Percent of litter-^{15}N that was recovered in the plant, microbial biomass, or litter-soil (excluding microbial biomass) when AMF were present (AMF Permitted) or excluded (AMF Excluded) (± standard error, n = 5). Data are for the final harvest (Day 70).

^{15}N Location	AMF Permitted	AMF Excluded	p value
Plant Total	4.89% ± 0.33	0.05% ± 0.06	<0.001
Shoot	*3.41% ± 0.23*	*0.01% ± 0.02*	*<0.001*
Root	*1.48% ± 0.48*	*0.04% ± 0.04*	*0.02*
Microbial Biomass	5.50% ± 0.28	5.84% ± 0.71	ns
Litter-Soil	36.76% ± 3.66	39.86% ± 2.97	ns
^{13}C:^{15}N in Soil	28.64 ± 0.52	27.08 ± 0.42	0.05

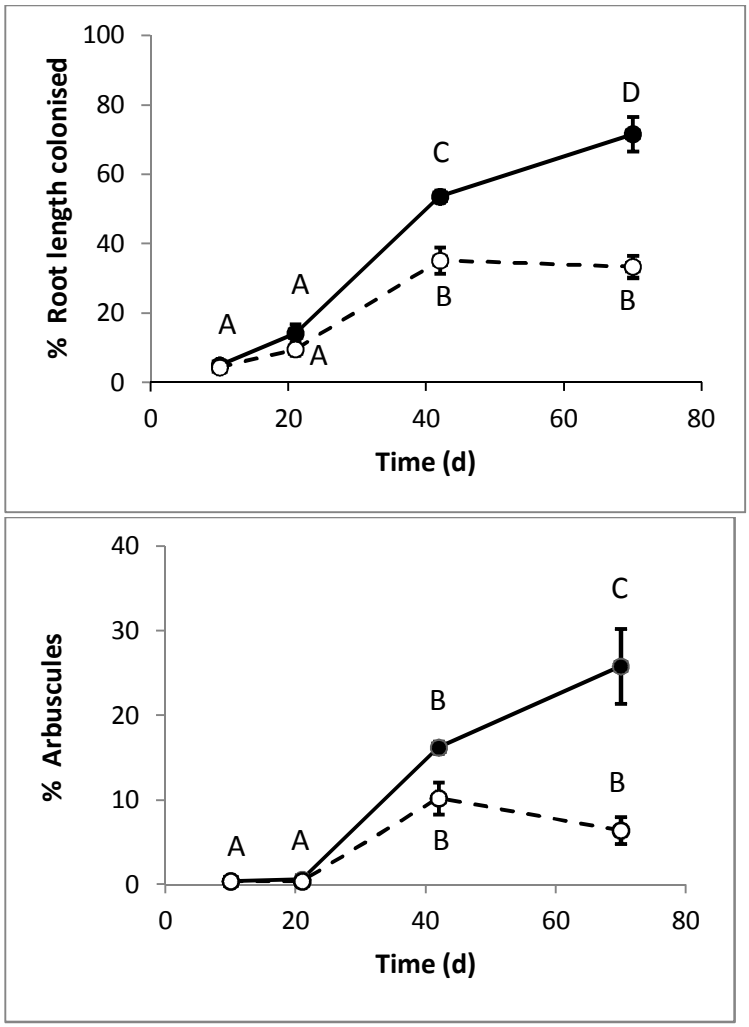

Supplemental Figure 1: (A) Percent root length colonized (RLC) and (B) percent arbuscules detected on *P. lanceolata* roots in the planted chamber for the AMF Permitted (closed circles) and AMF Excluded treatments (open circles)) (± SE). Letters indicate significant differences between the timepoints and treatments by Tukey HSD post-hoc analysis.

Supplemental Table 1: Richness of the taxa that significantly increased or decreased in relative abundance (RA) in response to the presence of AMF. Taxa are bacterial except when prefixed by (A) to signify archaea.

Phylum	Subphylum/Class	Family	(+RA)	(-RA)
Methanomicrobia (A)	Methanosarcinales	Methanosarcinaceae	0	1
AC1	Unclassified	Unclassified	1	0
Acidobacteria	Acidobacteriae	Unclassified	0	3
	iii1-15	Unclassified	1	0
	iii1-8	Unclassified	1	0
	RB25	Unclassified	1	0
	Solibacteres	Solibacteraceae	1	0
		Unclassified	1	2
Actinobacteria	Acidimicrobidae	Unclassified	1	3
	Actinobacteridae	Actinomycineae	0	1
		Arthrobacter	1	1
		Frankineae	1	0
		Gordoniaceae	0	3
		Intrasporangiaceae	0	2
		Micromonosporaceae	0	3
		Nocardiaceae	0	1
		Propionibacterineae	0	10
		Rhodococcus	1	0
		Streptomycineae	0	2
		Streptosporangineae	0	17
		Unclassified	2	9
	Coriobacteridae	Eggerthella	0	1
	WCHB1-81	Unclassified	0	1
Bacteroidetes	Bacteroidales	Bacteroidaceae	0	3
		Porphyromonadaceae	0	1
		Proteophilaceae	0	1
		Unclassified	0	2
	Flavobacteriales	Cytophaga	0	1
		Sporocytophaga	0	6
		Unclassified	1	1
	Flexibacterales	Algoriphagaceae	0	1
		Cytophaga	1	0
		Flexibacter	0	1
	Hymenobacterales	Hymenobacteraceae	0	1
	LD1	Unclassified	0	1
	p-184-o5	Unclassified	0	3
	Pochenobacter	Pochenobacter	1	0
	Saprospirales	Saprospiraceae	1	1
Chlorobi	BSV19	Unclassified	1	0
	OPB56	Unclassified	1	0
Chloroflexi	Anaerolineae	Anaerolineae	1	1
	Chloroflexi-4	Unclassified	0	1
	Dehalococcoidetes	Unclassified	2	0
Cyanobacteria	Nostoc	Nostoc	0	1

	Stigonematales	Unclassified	0	1
Cyanobacteria (cont.)	Unclassified	Unclassified	0	1
Deferribacteres	Deferribacter	Deferribacter	1	0
Firmicutes	Acidaminococcaceae	Acidaminococcaceae	1	0
	Alicyclobacillus	Alicyclobacillus	2	0
	Bacilli	Bacillus	1	0
		Exiguobacterium	1	0
		Halobacillus	2	0
		Marinococcus	1	0
		Paenibacillaceae	1	0
		Unclassified	9	1
	Clostridia	Acetivibrio	2	0
		Clostridiaceae	1	1
		Eubacterium	1	0
		Peptostreptococcaceae	1	1
		RF6	1	0
		Ruminococcus	1	0
		Unclassified	5	3
	Desulfotomaculum	Desulfotomaculum	1	0
	Mollicutes	Clostridium	1	0
		Unclassified	1	0
	Unclassified	Unclassified	0	1
Gemmatimonadetes	Gemm-4	Unclassified	1	0
	Gemm-1b	Unclassified	3	0
	Gemm-5	Unclassified	1	0
	Gemmatibacter	Unclassified	1	0
Haloanaerobiales	Halanaerobiaceae	Halanaerobiaceae	0	1
Marine_group_A	Unclassified	Unclassified	0	1
Nitrospirae	Thermodesulfovibrionales	Thermodesulfovibrionaceae	1	0
OP3	PBS-25	Unclassified	1	0
OP8	OP8-1	Unclassified	1	0
Planctomycetes	Planctomycetacia	Unclassified	4	1
	Unclassified	Unclassified	1	0
	WPS-1	B86	1	0
Proteobacteria	Alphaproteobacteria	Acetobacteraceae	0	1
		Bartonellaceae	0	1
		Beijerinckiaceae	0	1
		Bradyrhizobium	0	1
		Brevundimonas	0	2
		Hyphomicrobium	0	1
		Methylobacteriaceae	0	1
		Methylobacterium	2	0
		Nordella	1	0
		Phyllobacteriaceae	0	1
		Rhodoplanaceae	0	2
		Sphingomonas	0	2
		Stappia	0	2
		Unclassified	8	10
	Betaproteobacteria	Accumulibacter	0	1

		Alcaligenaceae	0	1
		Azoarcus	0	1
	Betaproteobacteria (cont.)	Burkholderiaceae	1	1
		Comamonadaceae	1	32
		Janthinobacterium	1	1
		mle1-7	1	0
		Nitrosomonadaceae	0	3
		Oxalobacteraceae	0	1
		Ralstoniaceae	0	2
		Unclassified	1	28
	Deltaproteobacteria	Desulfobacteraceae	2	0
		Desulfobacterium	1	0
		Geobacter	0	1
		Myxococcus	1	2
		Polyangiaceae	1	0
		Syntrophaceae	2	1
		Unclassified	5	3
	Desulfovibrionales	Desulfovibrionaceae	1	0
	Epsilonproteobacteria	Campylobacteraceae	1	0
		Helicobacteraceae	1	0
		Sulfuricurvaceae	0	1
		Sulfurospirillaceae	1	0
		Unclassified	1	0
	Gammaproteobacteria	Alteromonas	1	0
		Cellvibrio	0	1
		Chromatiaceae	0	1
		Colwelliaceae	0	1
		Enterobacteriales	1	3
		Halothiobacillaceae	0	1
		Methylococcaceae	0	2
		Microbulbifer	0	1
		Nevskiaceae	1	0
		Oceanimonaceae	0	1
		Piscirickettsiaceae	0	1
		Pseudomonadaceae	16	17
		Reinekea	0	1
		Rheinheimeraceae	0	1
		Stenotrophomonas	0	1
		Unclassified	1	13
		Vibrionaceae	1	0
Spirochaetes	Leptospirales	Leptonemaceae	1	0
	Spirochaetales	Spirochaetaceae	1	0
Synergistetes	Synergistes	Synergistes	0	1
	Thermovirga	Thermovirga	1	0
	Unclassified	Unclassified	1	0
TM7	TM7-3	Unclassified	1	0
Unclassified	Unclassified	Unclassified	2	0
Verrucomicrobia	Opitutae	Opitutaceae	0	2
WCHB1-27	Unclassified	Unclassified	1	0

WPS-2	Unclassified	Unclassified	1	0
ZB3	Unclassified	Unclassified	1	0
Grand Total			**134**	**250**

Supplemental Table 2: Richness of all taxa detected grouped by Phylum. To meet the detection criteria, each OTU needed to be detected in a minimum of three microarray replicates for at least one treatment.

Domain	Phylum	OTUs Detected	Domain	Phylum	OTUs Detected
Archaea	Halobacteria	5	Bacteria (cont.)	NC10	1
	Methanococci	1		Nitrospirae	8
	Methanomicrobia	7		NKB19	1
	MSBL1	3		OP10	3
	Thaumarchaeota	7		OP3	5
Bacteria	ABY1_OD1	1		OP8	3
	AC1	1		OP9_JS1	3
	Acidobacteria	89		Planctomycetes	38
	Actinobacteria	543		Proteobacteria	1786
	AD3	2		SC4	5
	Bacteroidetes	354		SPAM	1
	BRC1	3		Spirochaetes	47
	Caldithrix_KSB1	6		Sulfobacilli	2
	CD12	1		Synergistetes	6
	Chlamydiae	1		Thermi	6
	Chlorobi	20		Thermoanaerobacteria	1
	Chloroflexi	34		Thermodesulfobacteria	2
	Cyanobacteria	54		Thermosulfidobacterium	1
	Deferribacteres	3		Thermotogae	1
	Desulfitobacter	1		TM6	2
	Elusimicrobia_TG1	7		TM7	3
	Entotheonella	1		Unclassified	6
	Fibrobacteres	4		Verrucomicrobia	38
	Firmicutes	616		VHS-B3-43	1
	Fusobacteria	2		WCHB1-27	4
	Gemmatimonadetes	13		WPS-2	2
	GN02	2		WS3	9
	Haloanaerobiales	2		WS5	1
	Kazan-3B-22	1		WS6	1
	Lentisphaerae	2		ZB3	3
	Marine_group_A	7	Unclassified	Unclassified	5
	MVP-15	1			
	Natronoanaerobium	2	**Total**		3791